

Boundary layer control on convective available potential energy: Implications for cumulus parameterization

Leo J. Donner

Geophysical Fluid Dynamics Laboratory, NOAA, Princeton University, Princeton, New Jersey, USA

Vaughan T. Phillips

Program in Atmospheric and Oceanic Sciences, Princeton University, Princeton, New Jersey, USA

Received 13 May 2003; revised 1 August 2003; accepted 2 September 2003; published 22 November 2003.

[1] Convective available potential energy (CAPE), frequently regarded as an indicator of the potential intensity of deep convection, is strongly controlled by the properties of the planetary boundary layer (BL). Variations in CAPE observed during field experiments in midcontinent North America, the tropical east Atlantic, and the tropical west Pacific, can be accounted for mostly by changes in the temperature and humidity in the BL. The coupling between CAPE and the BL holds for both convective and nonconvective conditions. The coupling under conditions of deep convection implies a constraint on the intensity of deep convection which can be used as a closure for cumulus parameterization. This constraint requires equilibrium in the environment of the parcel used as a basis for calculating CAPE. Over many cases, parcel-environment equilibrium is observed to hold more robustly than equilibrium of CAPE itself. When observational uncertainties are considered, it is uncertain whether quasi-equilibrium, in which the rate of change of CAPE is substantially less than the rate at which mean advection and BL fluxes change CAPE, holds at subdiurnal timescales in the eastern Atlantic and the western Pacific. Quasi-equilibrium is a poor approximation at subdiurnal timescales in midcontinent North America. At timescales approaching diurnal, quasi-equilibrium holds in all cases. Cumulus parameterizations based on quasi-equilibrium may be limited in their ability to model diurnal cycles as a result. CAPE fluctuations related to large, subdiurnal variations in surface fluxes are much sharper than CAPE fluctuations related to changes in mean advection above the BL, especially over land. The strong BL control on CAPE indicates that deep convection does not equilibrate rapid, high-amplitude variations in CAPE originating there. *INDEX TERMS*: 3307 Meteorology and Atmospheric Dynamics: Boundary layer processes; 3314 Meteorology and Atmospheric Dynamics: Convective processes; 3319 Meteorology and Atmospheric Dynamics: General circulation; 3337 Meteorology and Atmospheric Dynamics: Numerical modeling and data assimilation; *KEYWORDS*: convective available potential energy, cumulus parameterization, planetary boundary layer

Citation: Donner, L. J., and V. T. Phillips, Boundary layer control on convective available potential energy: Implications for cumulus parameterization, *J. Geophys. Res.*, 108(D22), 4701, doi:10.1029/2003JD003773, 2003.

1. Introduction

[2] The interaction between cumulus convection and large-scale atmospheric flows remains a central, unsolved problem in atmospheric science. The strong links between convection, clouds, radiation, and water vapor imply that limitations in understanding this interaction remain a major source of uncertainty in understanding climate and climate change. Cumulus parameterizations represent the interaction between cumulus convection and mean flows in atmospheric general circulation models (GCMs). Cumulus parameterizations consist of both components which determine the

vertical distributions of sources and sinks of heat, moisture, chemical tracers, and horizontal momentum by convective systems and components which relate the intensity of convective systems to properties of the mean flow. The relationships between the intensity of convective systems and the properties of mean flows are referred to as closures.

[3] Many closures for cumulus parameterization are based on the broad concept that cumulus convection stabilizes a flow which has been destabilized by other processes acting on it. *Arakawa and Schubert* [1974] introduced the concept of quasi-equilibrium, which governs the rate at which the work done to an ensemble of cumulus parcels traveling from their cloud bases to their detrainment levels changes with time. This cloud work function is a measure of convective instability. For parcels which do not entrain

air from their environment, the cloud work function is the convective available potential energy (CAPE). As the mean flow changes, the cloud work function changes. Under quasi-equilibrium, convection occurs when mean advection and physical processes other than convection are destabilizing, and the net rate of change of cloud work function is much smaller than the rate at which mean advection and nonconvective physical processes act to increase it. An obvious means of satisfying quasi-equilibrium is for the intensity of deep convection to be just sufficient for the reduction in cloud work function by convection to balance the increase of cloud work function by mean advection and nonconvective physical processes (radiation, convergence of boundary layer and other small-scale turbulent fluxes, phase changes in nonconvective clouds). (For the purposes of this paper, convection will henceforth refer to deep convection.) A balance of this nature, in which absolute changes in CAPE are small, is referred to as “strict quasi-equilibrium” [Brown and Bretherton, 1997].

[4] Direct analyses of observations comparing the rate at which cloud work function, CAPE, or a generalization of CAPE (GCAPE, developed by Randall and Wang [1992]), changes to the rate at which these quantities change by mean advection and nonconvective physical processes have been reported. (GCAPE is the maximum energy obtained by any possible adiabatic rearrangement of parcels in a column.) Using data obtained in the Marshall Islands during Operation Redwing in 1956, Arakawa and Schubert [1974] find that the rate at which the cloud work function would change if only mean advection (advection of the mean temperature and moisture fields by the mean velocity) were acting is large relative to its net observed rate of change. Wang and Randall [1994] obtain similar results for GCAPE using GATE data. Zhang [2002], however, finds with ARM data that the net rate of CAPE change can be at least half as large as the CAPE change by mean advection and BL fluxes, with large sensitivity to his treatment of BL fluxes. Zhang [2003] extends this analysis to include the Tropical Ocean Global Atmosphere/Coupled Ocean-Atmosphere Response Experiment (TOGA-COARE) in the western Pacific and finds many cases in which the rate of CAPE change by mean advection and BL fluxes is not comparable to the rate at which it changes by cumulus processes at subdiurnal timescales. At longer timescales, these rates correspond more closely.

[5] In application, many cumulus parameterizations do not balance the rates of change of cloud work function due to mean advection and nonconvective parameterizations against convective parameterizations. Rather, the convective rate of change of cloud work function is balanced by the work function (possibly reduced by a threshold value) normalized by a relaxation time. Many applications do not use the cloud work function for an ensemble of clouds but use only CAPE. As examples, these approaches are used in the Community Atmospheric Model of the National Center for Atmospheric Research [Zhang *et al.*, 1998], the Geophysical Fluid Dynamics Laboratory AM2/LM2 (Geophysical Fluid Dynamics Laboratory Global Atmosphere Model Development Team, The GFDL new global atmosphere and land model AM2/LM2: Evaluation with prescribed SST simulations, sub-

mitted to *Journal of Climate*, 2003), HadAM3 of the Hadley Centre (using a low-level stability measure [Pope *et al.*, 2000]), and the European Centre for Medium-Range Weather Forecasts Integrated Forecasting System [Gregory *et al.*, 2000].

[6] Zhang [2002] uses field observations from the Atmospheric Radiation Measurement (ARM) program to examine the behavior of CAPE. Substantial variability in CAPE relative to its mean observed value during periods of convection is noted. Zhang [2002] finds that CAPE variation associated with the evolution of the troposphere above the BL is smaller than the complete variation of CAPE and proposes a closure for cumulus parameterizations based on this finding. The implication of these results is that CAPE evolution is substantially controlled by the evolution of the BL. These conclusions apply also to observations from the TOGA-COARE experiment [Zhang, 2003].

[7] Raymond [1995] and Emanuel [1995] propose “boundary layer quasi-equilibrium,” in which the BL is in an equilibrium between surface fluxes and downward fluxes of air from above the BL. The latter fluxes are generated by convection. This concept differs from that of Zhang [2002, 2003], which emphasizes variability in the BL as a source of CAPE variation. However, in the limit of “strict quasi-equilibrium,” Zhang’s [2002, 2003] equilibrium in CAPE variation associated with the evolution of the troposphere above the BL implies that “boundary layer quasi-equilibrium” also holds.

[8] The purpose of this paper is to examine boundary layer control on CAPE and its implications for closure for cumulus parameterization in oceanic tropical areas, as well as for the midlatitude continental location of ARM. CAPE is found to be under substantial control by the BL for the ARM site and for field programs in the east Atlantic and west Pacific. Sampling uncertainty renders uncertain whether quasi-equilibrium holds on timescales of hours for oceanic tropical areas. Quasi-equilibrium is unlikely to hold at these timescales for ARM. To the extent that CAPE is controlled by the BL, processes acting to modify CAPE outside of the BL are in approximate balance. For deep cumulus convection, this implies that changes in CAPE generated by mean advection and surface fluxes which converge above the BL are roughly balanced by convective processes above the BL. This balance can be used to close cumulus parameterizations, as noted by Zhang [2002, 2003]. Tests using this closure for the oceanic locations and the ARM site show that it holds more robustly than a balance of CAPE generation by mean advection and BL fluxes and CAPE destruction by convective processes in which BL contributions to CAPE tendencies are included. Apparently, large-amplitude, high-frequency variations in CAPE induced by surface fluxes are not balanced by convectively induced changes in CAPE. Large-amplitude, high frequency forcing is concentrated in the BL, where surface fluxes exert a strong influence, accounting for the more robust, limited balance among processes outside the BL.

2. Observational Analyses

[9] Three geographical regions are analyzed: central Oklahoma (ARM), cases A (27 June–1 July 1997),

B (8–13 July 1997) and C (13–18 July 1997); eastern Atlantic (GATE, Global Atmospheric Research Program Atlantic Tropical Experiment), 30 August–18 September 1974; and western Pacific (TOGA-COARE), 20–26 December 1992. Temperature and moisture analyses for ARM are obtained using constrained variational analysis [Zhang and Lin, 1997; Zhang *et al.*, 2001], as are surface fluxes. The corresponding GATE analyses and surface fluxes follow Thompson *et al.* [1979]. TOGA-COARE analyses of temperature and moisture are from Ciesielski *et al.* [1997]. Two sets of surface fluxes are used for TOGA-COARE, buoy data from Lin and Johnson [1996] and satellite estimates from Curry *et al.* [1999]. For ARM, GATE, and TOGA-COARE, the surface fluxes are used in conjunction with the BL parameterization in the Weather Research and Forecasting (WRF) model (<http://wrf-model.org>) to estimate the heating and moistening due to convergence of surface and eddy fluxes throughout the column [Troen and Mahrt, 1986; Hong and Pan, 1996].

[10] CAPE, defined here as the energy released by a parcel between the level of free convection and the level of zero buoyancy, is calculated using a starting level 35 hPa above the surface and a vertical increment of .09 hPa. (The vertical resolution corresponds to 10^4 vertical levels for the CAPE calculation, and the starting level is typically in the lower third of the BL.) Temperature and moisture are interpolated to this resolution from their coarser resolutions in the analyses. Finite time differences are taken over 3-hour intervals for GATE and ARM; 6-hour intervals for TOGA-COARE.

3. Boundary Layer Control on CAPE

[11] CAPE is the vertical integral between the level of free convection, p_{LFC} , and the level of zero buoyancy, p_{LZB} , of the density temperature difference between a parcel lifted without dilution from the BL and its large-scale environment:

$$CAPE = \int_{p_{LZB}}^{p_{LFC}} R_d (T_{\rho p} - T_{\rho}) d \ln p. \quad (1)$$

The density temperature T_{ρ} is defined as

$$T_{\rho} = T \frac{1 + q/\epsilon}{1 + q_T}, \quad (2)$$

where ϵ is the ratio of molecular weights of water to dry air and q_T is the total water mixing ratio. Condensate effects on temperature are not treated here. Pressure is denoted as p , density, ρ ; water vapor mixing ratio q , and the ideal gas constant for dry air, R_d . The subscript p on $T_{\rho p}$ indicates a property for an undilute parcel rising from the BL. All other variables refer to analyzed variables taken as representative of the mean flow or mean variables derived from the analyzed variables.

[12] Since the density temperature of the parcel is a function of the mean temperature and mixing ratio in the BL, the time (t) derivative of CAPE for a column in which

temperature and mixing ratio are measured in the BL (T_{BL} , q_{BL}) and on N discrete levels above the BL is

$$\begin{aligned} \frac{dCAPE}{dt} = & \frac{\partial CAPE}{\partial T_{BL}} \frac{\partial T_{BL}}{\partial t} + \frac{\partial CAPE}{\partial q_{BL}} \frac{\partial q_{BL}}{\partial t} + \sum_{k=1}^N \frac{\partial CAPE}{\partial T_k} \frac{\partial T_k}{\partial t} \\ & + \sum_{k=1}^N \frac{\partial CAPE}{\partial q_k} \frac{\partial q_k}{\partial t}. \end{aligned} \quad (3)$$

As noted by Zhang [2002], (3) can be written more compactly as

$$\frac{dCAPE}{dt} = \partial_t CAPE_{BL} + \partial_t CAPE_{PE}. \quad (4)$$

$\partial_t CAPE_{BL}$ refers to the sum of the first two terms on the right of (3), and $\partial_t CAPE_{PE}$ refers to the sum of the last two terms on the right of (3). The effect of time variations in the BL is measured by $\partial_t CAPE_{BL}$. The effect of variations above the BL (changes in the parcel environment) is measured by $\partial_t CAPE_{PE}$. Figures 1a–1c show $\frac{dCAPE}{dt}$ and $\partial_t CAPE_{BL}$ for observations from ARM, GATE, and TOGA-COARE. The observations are classified as convective if the precipitation rate is nonzero and $\frac{Q_1}{c_p}$ exceeds 5 K day^{-1} at any height between 5 and 10 km above ground level. The apparent heat source Q_1 is defined as

$$Q_1 = \frac{\partial s}{\partial t} + \nabla \cdot (\mathbf{v}s) + \frac{\partial(\omega s)}{\partial p}, \quad (5)$$

where s is the dry static energy, \mathbf{v} is the horizontal velocity, and ω is the vertical pressure velocity.

[13] The striking result in Figures 1a–1c is the dominance of $\partial_t CAPE_{BL}$ in determining $\frac{dCAPE}{dt}$ for both convective and nonconvective cases. Figures 1d–1f show time series of $\frac{dCAPE}{dt}$, $\partial_t CAPE_{BL}$, and $\partial_t CAPE_{PE}$. Again, CAPE variations are clearly controlled primarily by variations in the BL. CAPE variations due to changes in the parcel environment are generally relatively small. These results confirm the behavior noted by Zhang [2002, 2003] for ARM and TOGA-COARE but show that it also holds in an additional tropical oceanic environment, the east Atlantic. Yano *et al.* [2001] also find that CAPE variations in TOGA-COARE are largely accounted for by variations in the BL. Additional confirmation from a different geographical region is provided by McBride and Frank [1999], who find that day-to-day variations in CAPE observed in the Australian Monsoon Experiment are closely linked to BL equivalent potential temperature.

[14] Figures 1d–1f show that on subdiurnal timescales, the BL is not in equilibrium. Raymond [1995] postulates “boundary layer quasi-equilibrium” but asserts that it holds in the west Pacific on timescales of one-half of a day or greater. On these longer timescales, Figures 1d–1f show that many of the fluctuations in $\frac{dCAPE}{dt}$ cancel, and the BL is closer to equilibrium.

4. Quasi-Equilibrium

[15] The strong control over CAPE variations by the BL indicates aspects of CAPE behavior that are not obviously consistent with quasi-equilibrium. In particular, it empha-

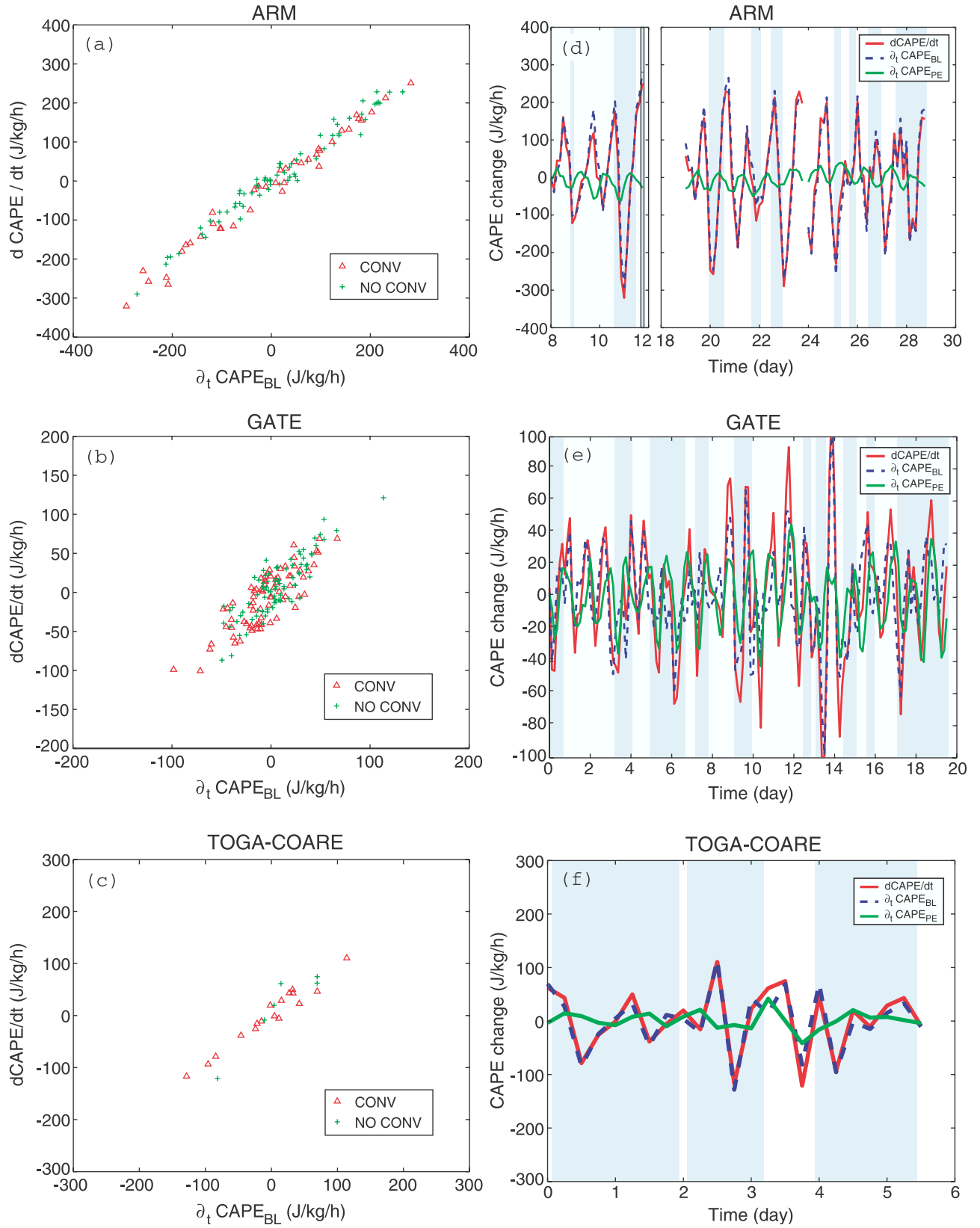


Figure 1. $\frac{dCAPE}{dt}$ and $\partial_t CAPE_{BL}$ for (a) ARM, (b) GATE, and (c) TOGA-COARE. Time series of $\frac{dCAPE}{dt}$, $\partial_t CAPE_{BL}$, and $\partial_t CAPE_{PE}$ for (d) ARM, (e) GATE, and (f) TOGA-COARE. Shading indicates periods of deep convection.

sizes variability. Under the quasi-equilibrium hypothesis, the rate at which CAPE changes due to advection by the mean velocity field and nonconvective physical processes is much greater than the net rate of CAPE change. Quasi-equilibrium thus allows for CAPE variations. The observations used to examine control on CAPE by the BL can also be used to examine quasi-equilibrium.

[16] Although GCMs have distinct parameterizations for convective and nonconvective processes, these processes in the atmosphere are so tightly coupled that the distinction between them is ambiguous. As noted by *Randall et al.* [1997], the subjective nature of the decomposition between convective and nonconvective processes is a weakness of the quasi-equilibrium construct. The analysis here groups CAPE variations due to mean advection of temperature and moisture and convergence of boundary layer fluxes of heat and moisture and compares them with the net rate of CAPE change. All phase changes are assumed to be convective, consistent with the observational evidence that in the presence of deep convection even stratiform clouds are produced to a large extent by convective detrainment [*Randall et al.*, 1997]. Radiation is not included. Since the analysis is restricted to convective time periods, for which $\frac{Q_1}{c_p}$ is required to exceed 5 K day^{-1} , the relative magnitude of radiative heating is generally small.

[17] The rate at which CAPE changes due to mean advection and boundary layer processes is calculated from the field observations as

$$\partial_t \text{CAPE}_{MABL} = \frac{\text{CAPE}(\tilde{T}, \tilde{q}) - \text{CAPE}(T, q)}{\Delta t} \quad (6)$$

where Δt is a time increment over which mean advection and BL fluxes operate. The temperature and mixing ratio incremented to account for large-scale processes, \tilde{T} and \tilde{q} , are

$$\tilde{T} = T + \partial_t T_{MA} \Delta t + \left(\frac{\partial T}{\partial t} \right)_{BL} \Delta t, \quad (7)$$

and

$$\tilde{q} = q + \partial_t q_{MA} \Delta t + \left(\frac{\partial q}{\partial t} \right)_{BL} \Delta t. \quad (8)$$

Boundary layer contributions are calculated as described in Section 2. The advective changes in temperature and water vapor by the mean velocity field are obtained from analyzed observations:

$$\partial_t T_{MA} = \frac{\partial T}{\partial t} - \frac{Q_1}{c_p}, \quad (9)$$

and

$$\partial_t q_{MA} = \frac{\partial q}{\partial t} + \frac{Q_2}{L}. \quad (10)$$

The apparent heat source is defined by (5), and L is the latent heat of vaporization. The apparent moisture sink is

$$Q_2 = -L \left[\frac{\partial q}{\partial t} + \nabla \cdot (\mathbf{v}q) + \frac{\partial(\omega q)}{\partial p} \right]. \quad (11)$$

[18] Figures 2a, 3a, and 4a contrast $\frac{d\text{CAPE}}{dt}$ and $\partial_t \text{CAPE}_{MABL}$ using observations averaged over 3h for ARM and GATE,

and averaged over 6 h for TOGA-COARE. (TOGA-COARE soundings were taken at 6-h intervals.) *Arakawa and Schubert* [1974] define quasi-equilibrium as an order-of-magnitude inequality, and it can be considered to hold if the $\frac{d\text{CAPE}}{dt}$ is an order of magnitude or more less than $\partial_t \text{CAPE}_{MABL}$. The ARM observations do not satisfy the quasi-equilibrium hypothesis. The GATE observations are more consistent with quasi-equilibrium. Using an analysis of sampling variability by *Mapes et al.* [2003], the uncertainty in the estimates of $\frac{d\text{CAPE}}{dt}$ can be estimated for TOGA-COARE. (Details of the error analysis are in Appendix A.) Many of the 6-h values of $\frac{d\text{CAPE}}{dt}$ for TOGA-COARE in Figure 4a are not an order of magnitude or more less than $\partial_t \text{CAPE}_{MABL}$, although the sampling variation is sufficiently large that standard deviations of these values in almost all cases extend to values that small. At best, it is ambiguous as to whether quasi-equilibrium holds at averaging times of 6 h for TOGA-COARE. If the timescale over which $\frac{d\text{CAPE}}{dt}$ and $\partial_t \text{CAPE}_{MABL}$ are averaged is increased, the observations become increasingly consistent with the quasi-equilibrium hypothesis. Figures 2c, 3c, and 4b compare $\frac{d\text{CAPE}}{dt}$ and $\partial_t \text{CAPE}_{MABL}$ for averaging times of 12 h, and Figures 2d, 3d, and 4c, for 24 h. For the latter averaging time, all of the cases considered satisfy the quasi-equilibrium hypothesis reasonably well even allowing for sampling variability in TOGA-COARE.

[19] At least for timescales of 24 h or longer, it is evident that viewing CAPE as under BL control and viewing CAPE as satisfying quasi-equilibrium are both reasonable. At shorter timescales over land surfaces, rapid variations in boundary layer properties can lead to CAPE variations which are comparable to CAPE variations associated with mean advection and BL processes. Diurnal variations can lead to rapid changes in surface properties, communicated by surface fluxes to the BL, as a source of these CAPE variations.

5. Implications for Closures in Cumulus Parameterizations

[20] An important application of these results on CAPE controls is closure for cumulus parameterization. As noted in Section 1, a common closure approach is to relax CAPE (or cloud work function) to a reference value over an adjustment time. The observations used to assess boundary layer control on CAPE and quasi-equilibrium in the previous sections can be used to assess closures of this nature, which can be expressed as

$$\partial_t \text{CAPE}_{Cu} = \frac{\text{CAPE}_0 - \text{CAPE}}{\tau}, \quad (12)$$

where τ is a relaxation time, and CAPE_0 refers to a reference value of CAPE.

[21] The rate at which CAPE is modified by cumulus convection, $\partial_t \text{CAPE}_{Cu}$, is estimated from observations as

$$\partial_t \text{CAPE}_{Cu} = \frac{\text{CAPE}(\tilde{T}, \tilde{q}) - \text{CAPE}(T, q)}{\Delta t}, \quad (13)$$

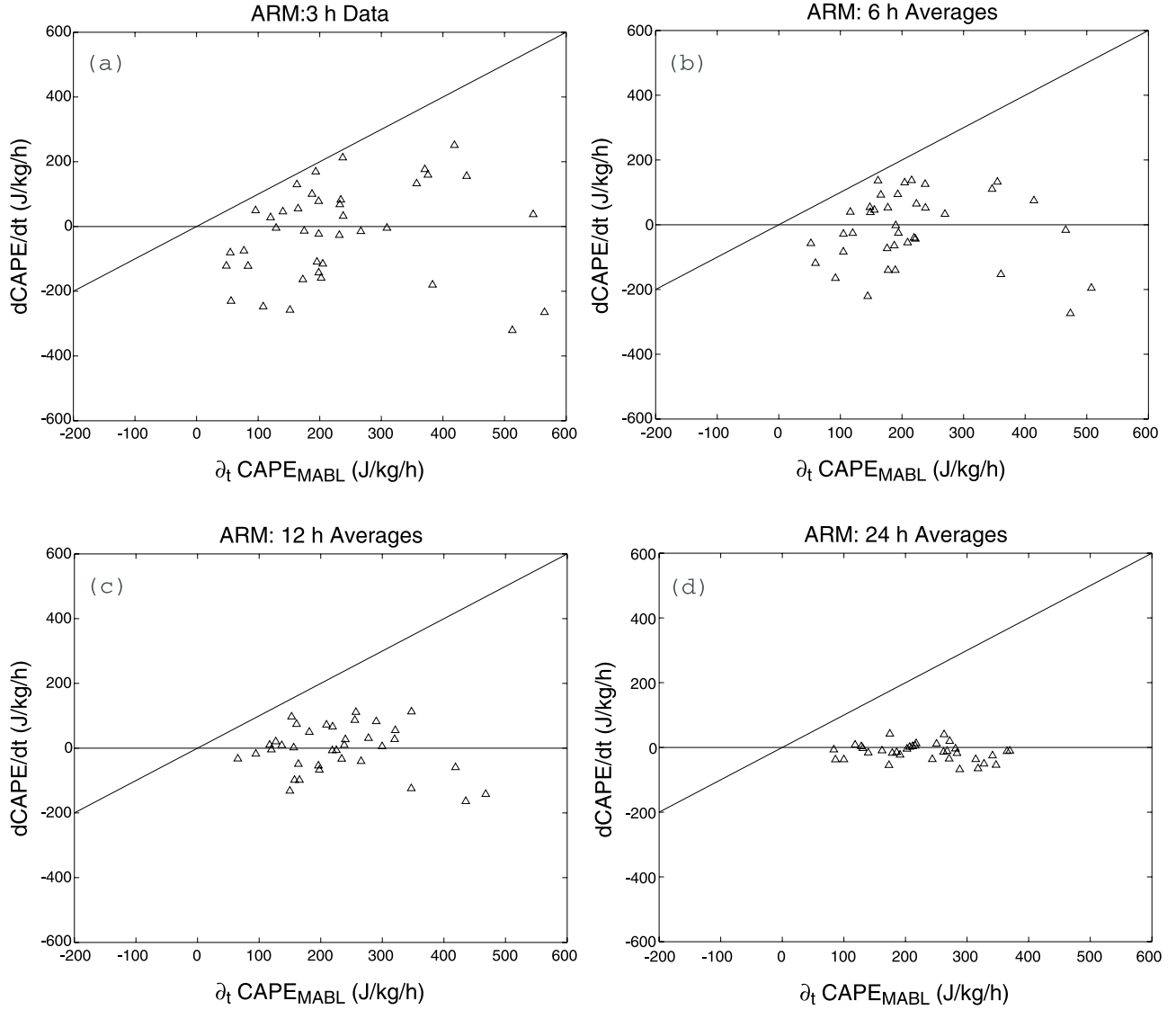


Figure 2. $\frac{dCAPE}{dt}$ and $\partial_t CAPE_{MABL}$ for ARM, for (a) 3 h, (b) 6 h, (c) 12 h, and (d) 24 h.

where

$$\tilde{T} = T + \left[\frac{Q_1}{c_p} - \left(\frac{\partial T}{\partial t} \right)_{BL} \right] \Delta t, \quad (14)$$

and

$$\tilde{q} = q - \left[\frac{Q_2}{L} + \left(\frac{\partial q}{\partial t} \right)_{BL} \right] \Delta t. \quad (15)$$

[22] Radiative heating is omitted in this approximation, and phase changes are assumed to be convective, as discussed in Section 4. Figure 5 shows a plot of $\partial_t CAPE_{Cu}$ and CAPE. Also indicated is an intercept-restricted least squares fit to (12). (The best fit intercept occurs at a negative value of CAPE, so $CAPE_0$ is chosen to be 0 for least squares.) The large scatter suggests (12) may be a problematic parameterization. Although the

TOGA-COARE subset of the observations may fit an expression of the form (12) well, a parameterization for general use would need to encompass at least the wider range of field programs in the other observations on Figure 5.

[23] “Strict quasi-equilibrium,” which could be used as a closure, asserts

$$\frac{dCAPE}{dt} = 0. \quad (16)$$

Note that quasi-equilibrium imposes a requirement on $\frac{dCAPE}{dt}$ relative to $\partial_t CAPE_{MABL}$ and does not demand that (16) hold. Indeed, Figures 1–4 show that CAPE variations driven by the BL are consistent with quasi-equilibrium, at least for sufficiently long timescales.

[24] In addition to the parameterization closures (12) and (16), an additional closure is suggested by Figure 1, which

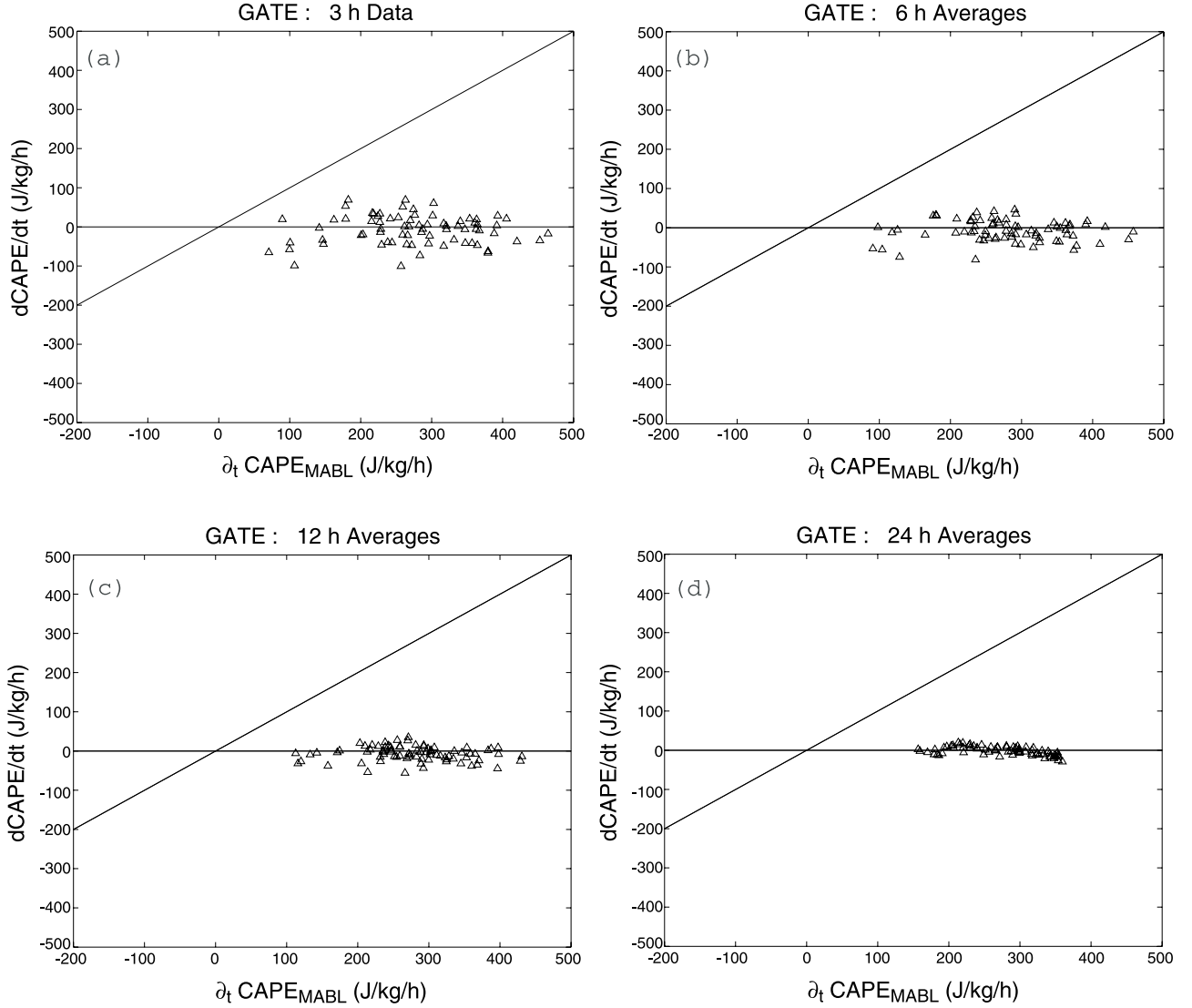


Figure 3. Same as Figure 2, except for GATE.

shows an approximate equality between $\frac{dCAPE}{dt}$ and $\partial_t CAPE_{BL}$. This equality, with (4), implies

$$\partial_t CAPE_{PE} = 0. \quad (17)$$

Zhang [2002, 2003] infer (17) based on ARM and TOGA-COARE data. Figure 1 confirms his ARM and TOGA-COARE results and extends them to the tropical east Atlantic.

[25] The closures (12), (16), and (17) are evaluated using convective-period observations from ARM, GATE, and TOGA-COARE in Figure 6. The frequency distributions show $\partial_t CAPE_{PE}$, $\frac{dCAPE}{dt}$, and $\partial_t CAPE_{Cu} + \frac{CAPE}{\tau}$. These quantities are predicted to be zero by the closures (17), (16), and (12), respectively, and the goodness of each closure is indicated by the narrowness of the peak in each distribution at zero. For ARM and GATE, the closure on $\partial_t CAPE_{PE}$ fits the observations best. For GATE, the CAPE-relaxation closure (12) is biased toward excessive CAPE consumption. Figures 1d–1f show the time histories of $\partial_t CAPE_{PE}$ and $\frac{dCAPE}{dt}$. The time histories confirm the

frequency distributions: $\partial_t CAPE_{PE}$ is consistently smaller than $\frac{dCAPE}{dt}$, although to a somewhat lesser degree for GATE than ARM and TOGA-COARE. Zhang [2002, 2003] finds the $\partial_t CAPE_{PE}$ closure to fit observations better than the $\frac{dCAPE}{dt}$ closure for ARM and TOGA-COARE. These calculations extend his results to the eastern Atlantic and show his closure to be more consistent with observations than CAPE relaxation for ARM and GATE but not TOGA-COARE.

[26] These closure results can be interpreted in terms of the tendencies of temperature due to mean advection and boundary layer flux convergence, $\partial_t T_{MA} + \left(\frac{\partial T}{\partial t}\right)_{BL}$, and mixing ratio, $\partial_t q_{MA} + \left(\frac{\partial q}{\partial t}\right)_{BL}$, shown for ARM B and TOGA-COARE in Figure 7. Lin and Johnson's [1996] buoy data are used to determine the boundary layer terms for Figures 7c and 7d.) For the continental ARM B, Figure 7 shows rapid, high-amplitude variations in the BL relative to the atmosphere above. Convection does not balance these variations, leading to BL control over CAPE. This imbalance also weakens “boundary layer quasi-equilibrium.” By excluding the BL, the closure (17) removes these sources of

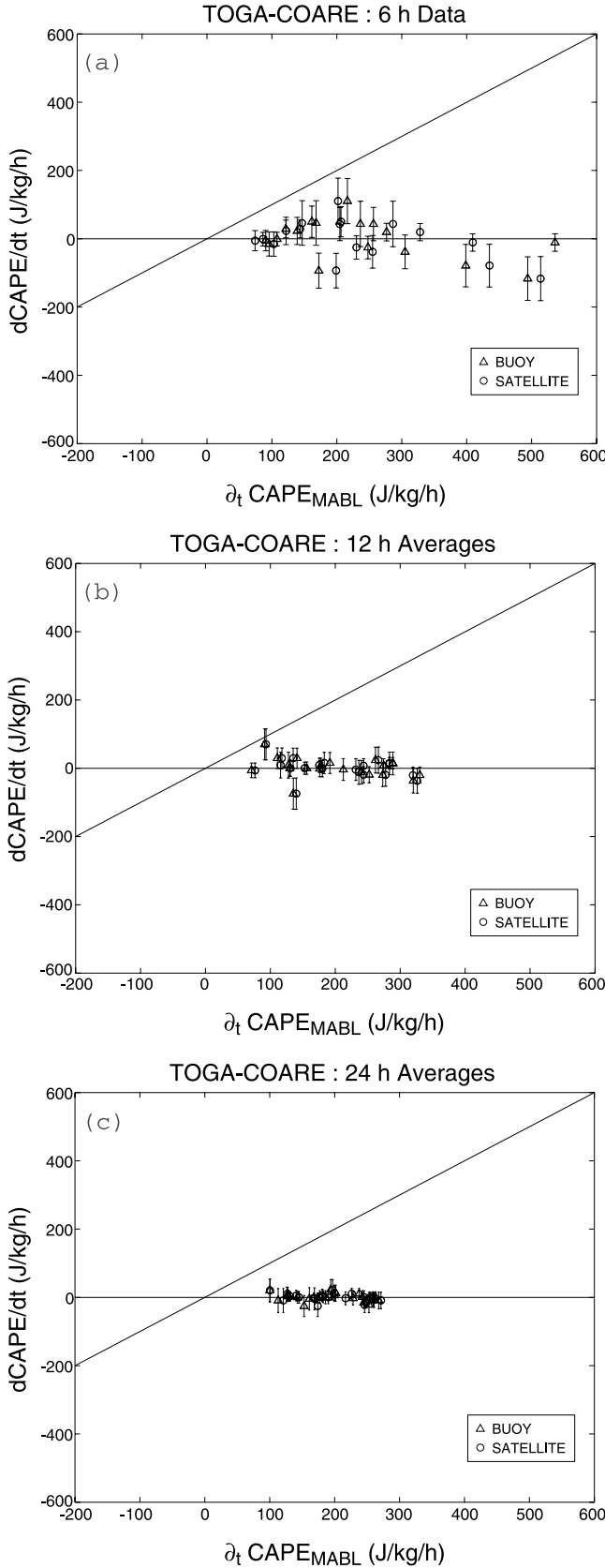


Figure 4. Same as Figure 2, except for TOGA-COARE and for (a) 6 h, (b) 12 h, and (c) 24 h.

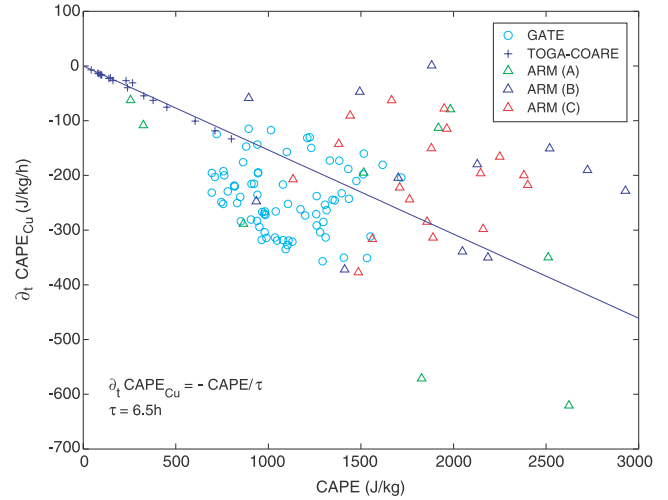


Figure 5. CAPE and $\partial_t CAPE_{Cu}$. The solid line is a least squares fit.

unbalanced CAPE variation, accounting for the better agreement with observation of (17) than (16). Figure 7 shows that large-amplitude, high-frequency components in the BL temperature and mixing-ratio tendencies are not as relatively pronounced in TOGA-COARE. Ocean temperatures, and thus surface fluxes, vary less for TOGA-COARE than for continental ARM B. ARM A and ARM C show behavior similar to ARM B. GATE shows behavior similar to TOGA-COARE.

[27] Figure 7 shows that BL flux convergence is generally large and concentrated. Smaller variability in these fluxes is associated with smaller values of $\frac{dCAPE}{dt}$. However, even at diurnal timescales, variations in BL flux prevent complete CAPE equilibrium. Figure 8 shows $\frac{dCAPE}{dt}$ and $\partial_t CAPE_{PE}$ calculated using 24-h averages. While both $\frac{dCAPE}{dt}$ and $\partial_t CAPE_{PE}$ tend toward smaller values at longer averaging times, equilibrium remains stronger for $\partial_t CAPE_{PE}$. *Brown and Bretherton* [1997] find that “strict quasi-equilibrium,” in which $\frac{dCAPE}{dt} = 0$, fails to hold even on monthly to interannual timescales, over which 25% variations in CAPE occur as a result of BL variations unlinked to those of the overlying troposphere. The diurnally averaged results in Figure 8 are consistent with their results, at much shorter timescales.

6. Conclusion

[28] Analysis of CAPE behavior in ARM, GATE, and TOGA-COARE indicates that temporal CAPE variations are controlled mostly by variations in the BL. For deep convection, this result corresponds to situations where convection is nearly balanced, except by processes associated with rapidly varying BLs. These CAPE variations are consistent with quasi-equilibrium if averaged over timescales longer than a substantial fraction of a day, suggesting that diurnal variability in surface fluxes, especially over land surfaces, produces large variations in the BL and CAPE.

[29] These results are useful in constructing closures for cumulus parameterizations. In particular, *Zhang’s* [2002] closure, which balances CAPE destruction by cumulus convection against CAPE generation by mean advection and convergence of surface fluxes above the BL, fits the

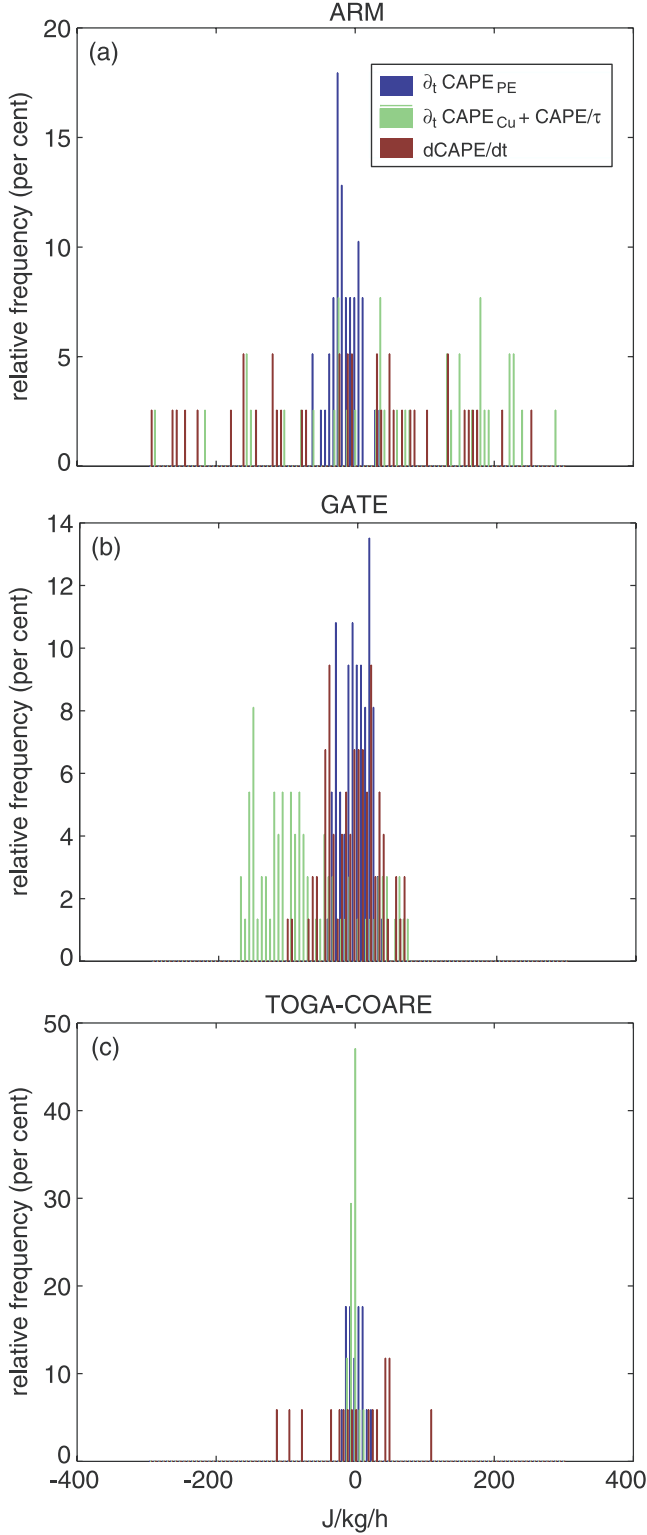


Figure 6. Frequency distribution of $\partial_t \text{CAPE}_{PE}$, $\frac{d\text{CAPE}}{dt}$, and $\partial_t \text{CAPE}_{Cu} + \frac{\text{CAPE}}{\tau}$ for (a) ARM, (b) GATE, and (c) TOGA-COARE. There are 100 equally spaced bins from -300 to $300 \text{ J kg}^{-1} \text{ hr}^{-1}$.

midlatitude continental and tropical oceanic observations analyzed here. The result that the closure on $\partial_t \text{CAPE}_{PE}$ fits observations better than the closure on $\frac{d\text{CAPE}}{dt}$ is not inconsistent with the observation that quasi-equilibrium holds.

While setting CAPE tendencies to zero for closure satisfies quasi-equilibrium trivially, it is not a unique means for doing so. These results suggest the $\frac{d\text{CAPE}}{dt}$ closure can be refined by using $\partial_t \text{CAPE}_{PE}$. The refined closure may be especially important in parameterizing diurnal variations of convection over land. Under these conditions, quasi-equilibrium does not hold well at subdiurnal timescales. Inaccurate closures at subdiurnal timescales can lead not only to inaccurate representation of phenomena at these timescales, but also (through nonlinear aspects of the interaction between convection, mean flows, and other physical processes) to inaccurate treatment of longer timescales as well.

[30] In cases where variations in the BL are small, e.g., midlatitudes during winter, the $\partial_t \text{CAPE}_{PE}$ closure reduces to “strict quasi-equilibrium,” i.e., vanishing $\frac{d\text{CAPE}}{dt}$. The analyses here suggest that, in general, multiple timescales operate for deep convection, mean flows, and the BL. Rapid variations in the BL are superposed on a slowly evolving balance between convection and mean advection. On timescales long enough for rapid variations in the BL to be smoothed, quasi-equilibrium holds.

[31] This analysis has used CAPE but could be equally well performed for cloud work functions with parcels that have nonzero entrainment. In general, entrainment will modify T_{pp} in (1) so that it depends in part on temperature and mixing ratio above the BL, increasing the dependence of entraining cloud work function (relative to CAPE) on temperature and mixing ratio above the BL. Variations in entraining cloud work function depend mostly on variations in the BL, and an equilibrium analogous to (17) for changes in entraining cloud work function produced by changes above the BL holds. For cumulus parameterizations which require closures on cloud work functions for several classes of clouds, these CAPE results apply directly to nonentraining (or nearly nonentraining) classes.

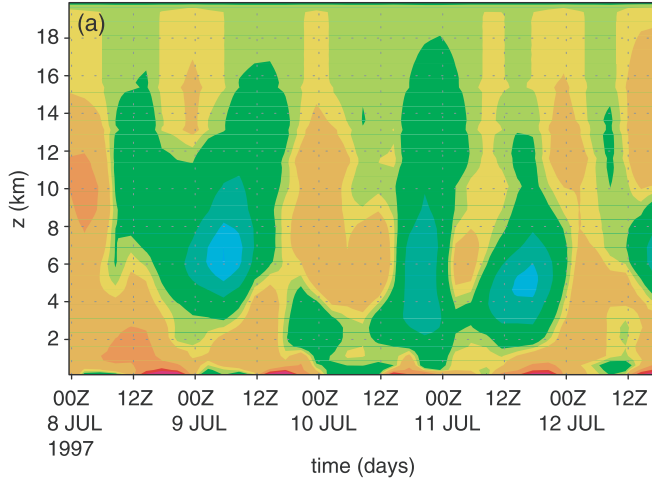
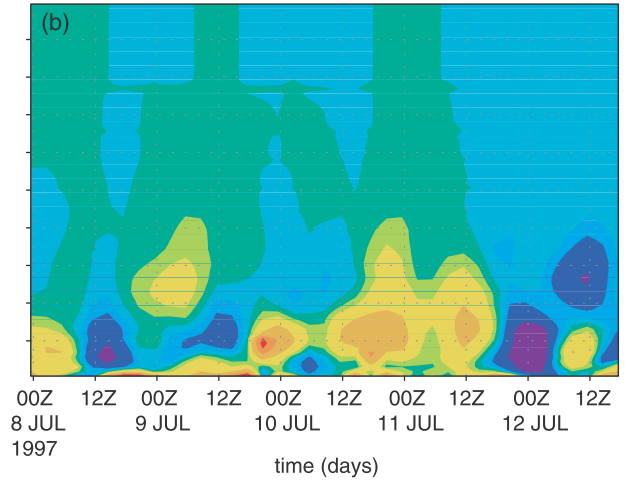
[32] This analysis has primarily considered convectively active cases. It does not address the separate issue of activation of convection or the factors which determine when convection occurs. These issues are also of obvious importance in the problem of cumulus parameterization.

[33] Although a refined closure for cumulus parameterization emerges from the analysis presented here, it is likely that this closure remains far from fundamentally correct. Underlying all of the closures discussed here, as well as those in general use in cumulus parameterization, is the notion that the large-scale averages of properties like CAPE and cloud work function are relevant in the sense that an idealized cumulus parcel interacts with an environment whose properties are those of the mean flow. In sharp contrast, studies with cloud-system resolving models [e.g., Donner *et al.*, 1999, Figure 8] show substantial spatial variations in CAPE on scales below that of the mean flow but greater than that of deep cumulus cells. Understanding the controls on these CAPE distributions is important in moving toward a more satisfactory basis for closing cumulus parameterizations.

Appendix A: CAPE Error Analysis

[34] Since CAPE is a nonlinear function of temperature and mixing ratio, a statistical model is constructed to infer the error in CAPE from the sampling uncertainty associated

ARM B

Temperature Tendency by Mean Advection
and BL Fluxes (K/day)Mixing-Ratio Tendency by Mean Advection
and BL Fluxes (g/kg/day)

TOGA-COARE

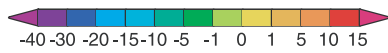
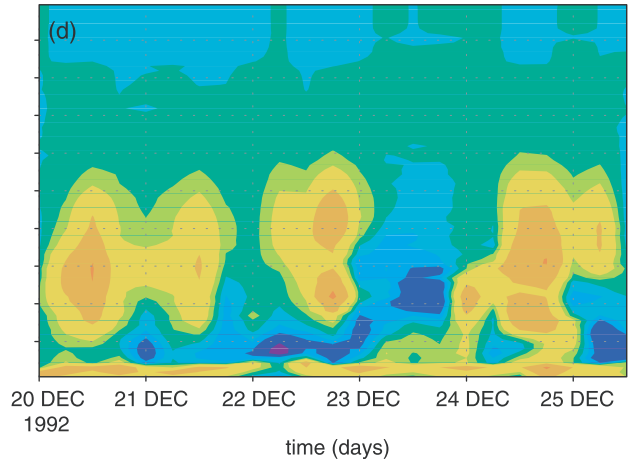
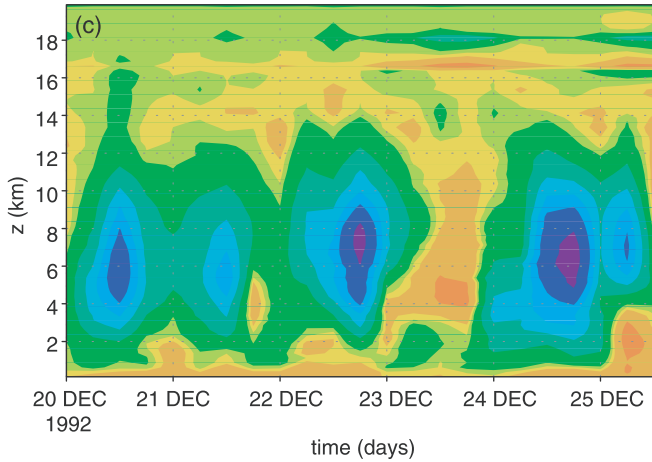


Figure 7. Tendencies due to mean advection and BL fluxes for temperature, $\partial_t T_{MA} + \left(\frac{\partial T}{\partial t}\right)_{BL}$, for (a) ARM B and (c) TOGA-COARE. Tendencies due to mean advection and BL fluxes for mixing ratio, $\partial_t q_{MA} + \left(\frac{\partial q}{\partial t}\right)_{BL}$, for (b) ARM B and (d) TOGA-COARE.

with unresolved spatial and temporal variability in temperature and mixing ratio. *Mapes et al.* [2003] observe that unresolved variability of relative humidity and temperature display vertical correlation scales of 100–200 hPa. Synthetic profiles of temperature and mixing ratio are generated by (1) dividing the depth of the atmosphere into 8 layers of thickness 100 hPa above a BL of thickness 200 hPa, and (2) drawing random perturbations from an independent normal distribution at the center of each layer and adding it to the observed array-average value, at that level. The relative humidity standard deviations are 2.5% below and 7.5% above the 600 hPa level, and the temperature standard deviation is .25 K. (These standard deviations apply to the 4-station TOGA-COARE array.)

[35] Within the BL, the same perturbations are applied at all heights. Above the BL, the perturbations vary linearly

between the centers of the layers, each of which has its own random distribution of perturbations. Any negative or super-saturated values generated by this process are set to zero or saturation, respectively. A sample of CAPE values is computed from 5000 synthetic profiles at each observation time. The variance of the CAPE is estimated from the variance of this sample. The variance of $\frac{dCAPE}{dt}$ is taken as the sum of the variances of the CAPE values used in the finite difference, divided by the time interval. When time averaging is performed, the array variances for temperature and humidity are divided by the number of observation times used to calculate the time average.

Notation

c_p specific heat at constant pressure, $\text{J kg}^{-1} \text{K}^{-1}$.
 $CAPE$ convective available potential energy, J kg^{-1} .

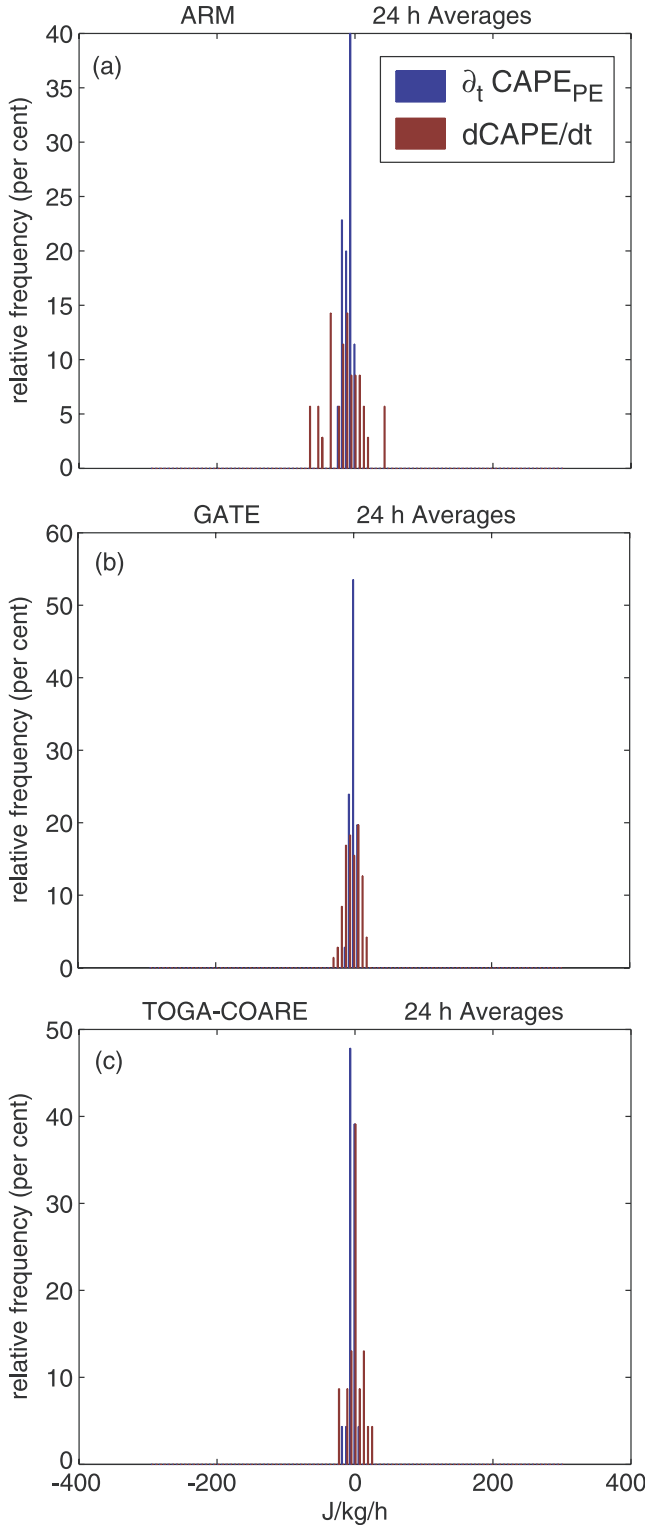


Figure 8. Frequency distribution of $\partial_t \text{CAPE}_{PE}$ and $\frac{d\text{CAPE}}{dt}$ for 24-h averaging time for (a) ARM, (b) GATE, and (c) TOGA-COARE.

- k vertical index, dimensionless.
- L latent heat of vaporization, J kg^{-1} .
- N number of vertical levels, dimensionless.
- p pressure, Pa.
- q vapor mixing ratio, $\text{kg (water) kg}^{-1}$.

- q_T total-water mixing ratio, $\text{kg (water) kg}^{-1}$.
- Q_1 apparent heat source, $\text{J kg}^{-1} \text{s}^{-1}$.
- Q_2 apparent moisture sink, $\text{J kg}^{-1} \text{s}^{-1}$.
- R_d gas constant for dry air, $\text{J kg}^{-1} \text{K}^{-1}$.
- s dry static energy, J kg^{-1} .
- t time, s.
- Δt time increment, s.
- T temperature, K.
- \mathbf{v} horizontal velocity, m s^{-1} .
- T_ρ density temperature, K.
- T_{pp} density temperature of lifted parcel, K.
- ϵ ratio of molecular weights, water to dry air, dimensionless.
- ω vertical (pressure) velocity, Pa s^{-1} .
- τ relaxation time, s.

The following apply generally:

- $()_{BL}$ refers to the planetary boundary layer.
- $()_{Cu}$ refers to cumulus convection.
- $()_{MA}$ refers to advection by the mean velocity field.
- $()_{LFC}$ refers to the level of free convection.
- $()_{LZB}$ refers to the level of zero buoyancy.
- $()_{PE}$ refers to parcel environment.
- $()_0$ refers to a reference or climatological value.
- $()$ refers to incremented values.

[36] **Acknowledgments.** Discussions with Dave Randall (Colorado State University), Guang Zhang (Scripps Institution of Oceanography), Jun-ichi Yano (CNRM Meteo France), and Olivier Pauluis (Princeton University) on quasi-equilibrium have been helpful in presenting the material in this paper. Charles Seman assisted in preparing analyses for use in this study. Steve Krueger (University of Utah) provided temperature and moisture analyses and surface fluxes for TOGA-COARE. Kuan-Man Xu (NASA Langley Research Center) provided GATE surface fluxes. Reviews by Steve Klein, Charles Seman, Brian Mapes, and anonymous reviewers have contributed to the development of the paper. Partial support has been provided by NASA Interagency Agreement IA1-553 (CERES).

References

- Arakawa, A., and W. H. Schubert, Interaction of a cumulus cloud ensemble with the large-scale environment: Part 1, *J. Atmos. Sci.*, **31**, 674–701, 1974.
- Brown, R. G., and C. S. Bretherton, A test of the strict quasi-equilibrium theory on long time and space scales, *J. Atmos. Sci.*, **54**, 624–638, 1997.
- Ciesielski, P. E., L. M. Hartten, and R. H. Johnson, Impacts of merging profiler and rawinsonde winds on TOGA COARE analyses, *J. Atmos. Oceanic Technol.*, **14**, 1264–1279, 1997.
- Curry, J. A., C. A. Clayson, W. B. Rossow, R. Reeder, Y.-C. Zhang, P. J. Webster, G. Liu, and R.-S. Sheu, High-resolution satellite-derived data set of the surface fluxes of heat, freshwater, and momentum for the TOGA COARE IOP, *Bull. Am. Meteorol. Soc.*, **80**, 2059–2080, 1999.
- Donner, L. J., C. J. Seman, and R. S. Hemler, Three-dimensional cloud-system modeling of GATE convection, *J. Atmos. Sci.*, **56**, 1885–1912, 1999.
- Emanuel, K. A., The behavior of a simple hurricane model using a convective scheme based on subcloud-layer entropy equilibrium, *J. Atmos. Sci.*, **52**, 3960–3968, 1995.
- Gregory, D., J.-J. Morcrette, C. Jakob, A. C. M. Beljaars, and T. Stockdale, Revision of convection, radiation, and cloud schemes in the ECMWF Integrated Forecasting System, *Q. J. R. Meteorol. Soc.*, **126**, 1685–1710, 2000.
- Hong, S.-Y., and H.-L. Pan, Nonlocal boundary layer vertical diffusion in a medium-range forecast model, *Mon. Weather Rev.*, **124**, 2322–2339, 1996.
- Lin, X., and R. H. Johnson, Heating, moistening, and rainfall over the western Pacific warm pool during TOGA COARE, *J. Atmos. Sci.*, **53**, 3367–3383, 1996.
- Mapes, B. E., P. E. Ciesielski, and R. H. Johnson, Sampling errors in rawinsonde-array budgets, *J. Atmos. Sci.*, **60**, 2697–2714, 2003.
- McBride, J. L., and W. M. Frank, Relationships between stability and monsoon convection, *J. Atmos. Sci.*, **56**, 24–36, 1999.

- Pope, V. D., M. L. Gallani, P. R. Rowntree, and R. A. Stratton, The impact of new physical parametrizations in the Hadley Centre climate model: HadAM3, *Clim. Dyn.*, *16*, 123–146, 2000.
- Randall, D. A., and J. Wang, The moist available energy of a conditionally unstable atmosphere, *J. Atmos. Sci.*, *49*, 240–255, 1992.
- Randall, D. A., D.-M. Pan, P. Ding, and D. G. Cripe, Quasi-equilibrium, in *The Physics and Parameterization of Moist Atmospheric Convection*, edited by R. K. Smith, pp. 359–385, Kluwer Acad., Norwell, Mass., 1997.
- Raymond, D. J., Regulation of moist convection over the west Pacific warm pool, *J. Atmos. Sci.*, *52*, 3945–3959, 1995.
- Thompson, R. M., S. W. Payne, E. E. Recker, and R. J. Reed, Structure and properties of synoptic-scale wave disturbances in the intertropical convergence zone of the eastern Atlantic, *J. Atmos. Sci.*, *36*, 53–72, 1979.
- Troen, I., and L. Mahrt, Simple model of the atmospheric boundary layer; sensitivity of surface evaporation, *Boundary Layer Meteorol.*, *37*, 129–148, 1986.
- Wang, J., and D. A. Randall, The moist available energy of a conditionally unstable atmosphere, II: Further analysis of the GATE data, *J. Atmos. Sci.*, *51*, 703–710, 1994.
- Yano, J.-I., K. Fraedrich, and R. Blender, Tropical convective variability as $1/f$ noise, *J. Clim.*, *14*, 3608–3616, 2001.
- Zhang, G., Convective quasi-equilibrium in midlatitude continental environment and its effect on convective parameterization, *J. Geophys. Res.*, *107*(D14), 4220, doi:10.1029/2001JD001005, 2002.
- Zhang, G., Convective quasi-equilibrium in the tropical western Pacific: Comparison with midlatitude continental environment, *J. Geophys. Res.*, *108*(D19), 4592, doi:10.1029/2003JD003520, 2003.
- Zhang, G. J., J. T. Kiehl, and P. J. Rasch, Response of climate simulation to a new convective parameterization in the National Center for Atmospheric Research Community Climate Model (CCM3), *J. Clim.*, *11*, 2097–2115, 1998.
- Zhang, M. H., and J. L. Lin, Constrained variational analysis of sounding data based on column-integrated budgets of mass, heat, moisture, and momentum: Approach and application to ARM measurements, *J. Atmos. Sci.*, *54*, 1503–1524, 1997.
- Zhang, M. H., J. L. Lin, R. T. Cederwall, J. J. Yio, and S. C. Xie, Objective analysis of ARM IOP data: Method and sensitivity, *Mon. Weather Rev.*, *129*, 295–311, 2001.

L. J. Donner, Geophysical Fluid Dynamics Laboratory, NOAA, P.O. Box 308, Princeton University, Princeton, NJ 08542, USA. (ljd@gfdl.noaa.gov)
V. T. Phillips, Program in Atmospheric and Oceanic Sciences, Princeton University, Princeton, NJ 08542, USA.